

# An Experimental Study of Transient Liquid Phase Bonding of the Ternary Ag-Au-Cu System Using Differential Scanning Calorimetry

M.L. KUNTZ, B. PANTON, S. WASIUR-RAHMAN, Y. ZHOU, and S.F. CORBIN

An experimental approach using differential scanning calorimetry (DSC) has been applied to quantify the solid/liquid interface kinetics during the isothermal solidification stage of transient liquid phase (TLP) bonding in an Ag-Au-Cu ternary alloy solid/liquid diffusion couple. Eutectic Ag-Au-Cu foil interlayers were coupled with pure Ag base metal to study the effects of two solutes on interface motion. Experimental effects involving baseline shift and primary solidification contribute to a systematic underestimation of the fraction of liquid remaining. A temperature program has been used to quantify and correct these effects. The experimental results show a linear relationship between the interface position and the square root of the isothermal hold time. The shifting tie line composition at the interface has been shown to affect the DSC results; however, the impact on the calculated interface kinetics has been shown to be minimal in this case. This work has increased the knowledge of isothermal solidification in ternary alloy systems and developed accurate experimental methods to characterize these processes, which is valuable for designing TLP bonding schedules.

DOI: 10.1007/s11661-013-1704-0

© The Minerals, Metals & Materials Society and ASM International 2013

## I. INTRODUCTION

TRANSIENT liquid phase (TLP) bonding<sup>[1,2]</sup> or diffusion brazing is a bonding process that has been developed to join materials which are otherwise very difficult to join.<sup>[3,4]</sup> The bonding process is a brazing or soldering variation that utilizes an interlayer that melts at a temperature lower than that of the substrate to form a liquid at the faying surface.<sup>[3]</sup> The TLP process is able to create high quality bonds by the resolidification of this liquid at a constant temperature.<sup>[3]</sup> This is made possible by the use of a melting point depressant (MPD)-rich interlayer which melts or reacts with the base metal to form a liquid upon heating through the liquidus of the braze alloy. In the liquid phase, the MPD (solute) will diffuse into the base metal (solvent). The resultant change in chemistry of the liquid phase will lead to isothermal solidification *via* epitaxial growth from the substrate.<sup>[5]</sup> A homogeneous bond similar to the bulk material will be created as the substrates of each side of the bond come in contact with one another at the joint centerline. This is much more ideal than the heterogeneous bond that results from solidification through cooling in traditional brazing processes. TLP bonding results in a bond of similar melting temperature

to the base metal, which has led to its use in high temperature applications.<sup>[6,7]</sup> The potential for creation of a high quality joint has sparked interest in the application of TLP for joining materials that have been found difficult to join using traditional fusion welding processes.<sup>[1,3,6-10]</sup> Practical application may be limited by several issues:

1. TLP bonding is controlled by the diffusion of the solutes into the solid solvent, which leads to a process time normally on the order of hours. Optimization of the process involves the reduction of the process time, while maintaining an acceptable quality.
2. Designing a TLP bonding process is timely and costly. Solidified joint cross sections are examined to estimate the width of the remaining eutectic liquid, but the results are often erroneous.<sup>[11]</sup>
3. Existing analytical models developed for prediction of isothermal solidification completion time are inaccurate, and the errors increase as polycrystallinity and multiphase alloy systems are introduced.<sup>[12-14]</sup>
4. Numerical modeling aided by commercial DIC-TRA/Thermocalc software can be used to increase prediction accuracy in binary and ternary systems.<sup>[15,16]</sup> Unfortunately, the models are complex and currently limited to lower-order component systems without the ability to predict kinetics in higher-order multicomponent systems used by TLP bonding schedule developers.

Current TLP process development techniques are timely, costly, and prone to errors. Existing models vary in inaccuracy and introduction of numerical methods limits use by TLP process developers. There is a need for

---

M.L. KUNTZ, Director of Engineering Research, B. PANTON and S. WASIUR-RAHMAN, Ph.D. Candidates, Y. ZHOU, Professor, and S.F. CORBIN, Adjunct Professor, are with the Department of Mechanical Engineering, University of Waterloo, 200 University Ave. W., Waterloo, ON N2L 3G1, Canada. Contact e-mail: nzhou@uwaterloo.ca

Manuscript submitted February 8, 2010.

a reliable experimental method necessary to quantify the isothermal solidification kinetics of the TLP process.

Corbin and Lucier<sup>[17]</sup> demonstrated the use of differential scanning calorimetry (DSC) to measure the process kinetics of the TLP sintering process. They showed that geometrical differences in the TLP bonding process can profoundly affect the DSC results and may require further analysis.<sup>[18]</sup> The kinetics of low-temperature TLP solidification in electroplated Au-Sn layers on a Cu substrate using DSC was studied by Venkatraman *et al.*<sup>[19]</sup> A semi-infinite width of base metal assumption was made in their model, which is invalidated by the thin width of the base metal used in their experiment. They showed a systematic underestimation of the fraction of liquid remaining after an isothermal hold period.<sup>[20]</sup> This underestimation has been shown to be due to the planar nature of the solid/liquid interface, an effect that can be corrected.<sup>[18]</sup>

The wealth of information available and the simplicity of binary systems have led to the majority of research investigating the measurement and prediction of isothermal solidification kinetics in these simple, single solute systems. These systems have limited application, so more effort is required to investigate ternary and higher systems. The additional solute elements complicate the isothermal solidification process. Complex numerical models have been developed to predict the kinetics of the solid/liquid interface.<sup>[21]</sup> The assumptions that form the basis of the models are critically deficient in experimental data evidence.<sup>[12,22]</sup> A method has been developed and verified by experimental data to quantify the kinetics of interface motion in a solid/liquid diffusion couple using differential scanning calorimetry (DSC).<sup>[18]</sup> The method has been successfully applied for characterization of isothermal solidification kinetics during TLP bonding in a binary Ag-Cu system.<sup>[11]</sup> In this work, the DSC method for measuring solid/liquid interface kinetics was applied to the isothermal solidification stage during TLP bonding of the ternary Ag-Au-Cu system.

## II. PROCESS DESCRIPTION

A review paper by Zhou *et al.* provides a detailed description of the TLP bonding process.<sup>[5]</sup> The four discrete stages of the TLP bonding process are 1. heating, 2. dissolution and widening, 3. isothermal solidification, and 4. homogenization.<sup>[5,9,23]</sup> Two variants of the process have been described by MacDonald and Eagar.<sup>[24]</sup> The category-A process uses a pure interlayer and the melting is controlled by diffusion of the MPD into the base metal.<sup>[24]</sup> The category-B process is more desirable because it uses an interlayer near the liquidus composition at the bonding temperature, typically a eutectic that theoretically instantaneously melts.<sup>[24]</sup> A theoretic description of the category-B process for a binary system has been presented by Kuntz *et al.*<sup>[11]</sup> Once the interlayer has melted and wetted the substrates, dissolution occurs where the width of the liquid layer will increase due to change in solidus/liquidus composition and mass balance requirements.

Once the maximum liquid width has been reached and the composition of the liquid is uniform, the MPD will diffuse into the base metal. The liquid composition remains at the liquidus composition of the isothermal temperature. As the solute diffuses out of the liquid, mass balance is maintained by shrinking of the liquid width *via* isothermal solidification. When the final solidification occurs, a solute peak with the solidus composition will be present at the centerline. A homogenization stage is used to minimize this peak through solid-state diffusion of the elements into the base material. The lengthiest portions of the process are the isothermal solidification and homogenization stages due to their dependence on solute diffusion into a solid.<sup>[25]</sup> This process will become more complex as more elements are added to the system.

For an isothermal, isobaric system, the Gibbs' phase rule seen in Eq. [1] predicts the degrees of freedom of a system ( $f$ ), which is related to the number of components ( $n$ ) and the number of phases ( $p$ ).<sup>[26]</sup>

$$f = n - p \quad [1]$$

In the binary case, there are zero degrees of freedom; however, in the ternary case, the additional component affords the system one degree of freedom. This allows isothermal solidification to proceed by way of a shifting liquid composition. The interaction between the two solutes generally results in the interfacial, local equilibrium concentrations shifting throughout the solidification process.<sup>[27]</sup> The isothermal solidification mechanism of the process in ternary systems is the diffusion of both solutes across the solid/liquid interface and into the base material. A mass balance can be written for each of the solutes in the system. The mass balance for each solute can be written as follows:

$$(C_{Lz,B} - C_{zL,B}) \cdot \frac{d}{dt} X(t) = D_B \cdot \frac{\partial}{\partial x} C_B(x, t)_{x=X(t)} \quad [2]$$

$$(C_{Lz,C} - C_{zL,C}) \cdot \frac{d}{dt} X(t) = D_C \cdot \frac{\partial}{\partial x} C_C(x, t)_{x=X(t)} \quad [3]$$

$C_{Lz}$  and  $C_{zL}$  are the liquid and solid concentrations, respectively, at the solid/liquid interface. The  $D_B$  and  $D_C$  are the diffusivity constants of  $B$  and  $C$ , respectively.  $B$  and  $C$  are the respective solutes. The concentration gradient in the liquid is assumed negligible. The interface velocities supported by each solute will be the same for only a limited number of cases. Since there can only be one single solid/liquid interface velocity, there must be some mechanism controlling the isothermal solidification behavior.

The Ag-Au-Cu ternary system will be considered to illustrate the potential isothermal solidification behaviors. The model consists of a pure semi-infinite base metal substrate (Ag) with a ternary eutectic interlayer of approximately Ag-14 at. pct Au-43 at. pct Cu. Upon heating, the interlayer will melt and dissolution will occur. The dissolution is controlled by diffusion in the liquid, so many systems differ little from binary dissolution kinetics.<sup>[26]</sup> If it

is assumed that no solid-state diffusion occurs during dissolution, then the dissolution will occur on a straight line from the initial interlayer composition to the pure base metal composition as shown on the Gibbs' isotherm in Figure 1.<sup>[26]</sup> The initial liquidus composition will lie at the intersection of this line and the liquid phase boundary on the Gibbs' isotherm for the bonding temperature.<sup>[26]</sup>

Sinclair *et al.*<sup>[27]</sup> have suggested that the interface velocity will be initially controlled by the solute that supports the faster velocity. The kinetics will be governed by the flux and equilibrium composition difference between the solid and liquid phase in Eqs. [2] and [3] that results in the fastest interface velocity. As the first solute diffuses into the solvent, the second solute must be partitioned back into the liquid to satisfy the conservation of mass. This results in the composition of the liquid moving along the liquidus line on the Gibbs' isotherm of the ternary equilibrium phase diagram. Figure 2 shows the dissolution path of the interlayer and subsequent shifting of the tie line during the isothermal solidification stage.

From this theory of isothermal solidification mechanics, there are a number of different situations that can occur as follows.

1. The composition of the liquid will continually shift until isothermal solidification is complete.<sup>[27]</sup>

2. If a special set of conditions exists in the system, there is a possibility of a "stationary case" where the composition of the liquid will remain constant throughout the isothermal solidification stage.<sup>[27]</sup>
3. In a combination of the previous two cases, the liquid composition may shift until a stationary condition exists.<sup>[27]</sup> These conditions are history dependent and will not be the same initial conditions that support the stationary case.

The Ag-Au-Cu system is theorized to isothermally solidify *via* the shifting tie line mechanism.

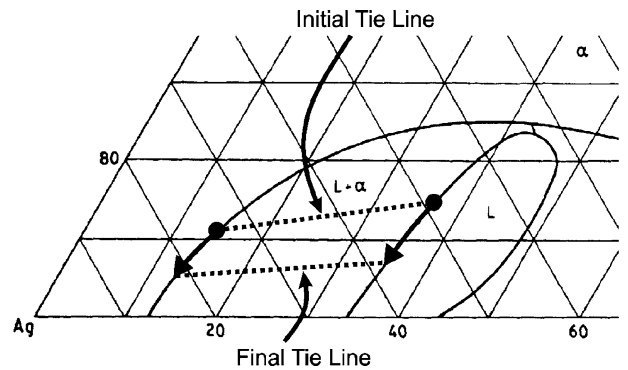


Fig. 2—Isothermal solidification *via* a shifting tie line in the 1073 K (800 °C) isotherm of the Ag-Au-Cu ternary system.<sup>[34]</sup>

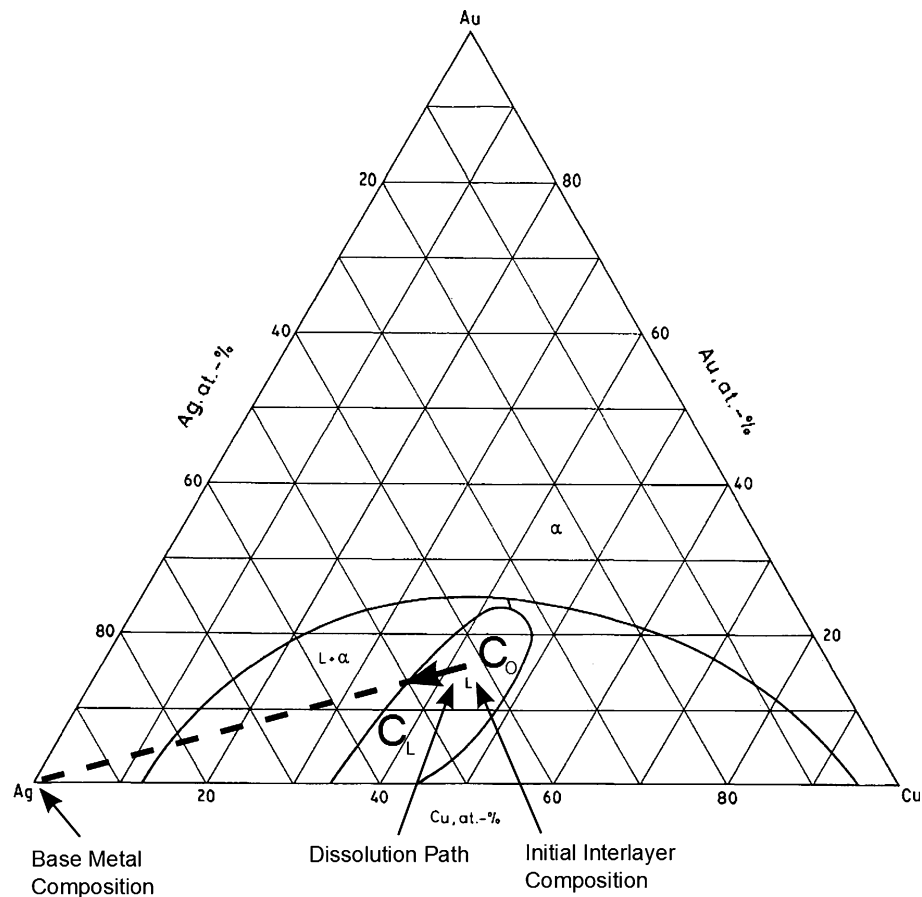


Fig. 1—Dissolution path of the interlayer in the 1073 K (800 °C) isotherm of the Ag-Au-Cu ternary system.<sup>[34]</sup>

### III. ANALYSIS OF A TERNARY DIFFUSION COUPLE

In the isothermal solidification process characteristic of TLP bonding, the addition of a second solute to the liquid increases the complexity of the material system. It is desirable to limit the difficulty of interpreting the interface kinetics by selecting a material system that is simple in nature. The liquidus projection of the Ag-Au-Cu system in Figure 3 shows that the addition of Au to the Ag-Cu binary system results in a system with a single ternary eutectic. The eutectic occurs at a composition of Ag-27 wt pct Au-27 wt pct Cu (Ag-14 at. pct Au-43 at. pct Cu) with a melting temperature of 1040 K (767 °C). The eutectic trough extends from the Ag-Cu binary eutectic along a line of nearly constant Cu composition.<sup>[28]</sup> The Ag-Au and Ag-Cu binary phase diagrams are both isomorphous.<sup>[29]</sup> The Au-Cu binary phase diagram is isomorphous at temperatures above 683 K (410 °C), showing miscibility gaps at lower temperatures.<sup>[30]</sup>

In the 1073 K (800 °C) isotherm shown in Figure 1, the system is composed of an isomorphous solid phase and a liquid phase which lends this system to be ideal for TLP bonding and simplifies the analysis of interface kinetics. The diffusivities of the components lead to reasonable experimentation time, and it is known that the effects of cross diffusion are nearly negligible within the composition range of interest.<sup>[31]</sup> They do not have tenacious oxides and Ag is considered noble in this

study because no stable oxide forms at the temperature of interest. Furthermore, studying this system could lead to potentially interesting results because the solidus phase boundary in the silver-rich region decreases in Au as Cu is decreased. This does not follow the model developed for isothermal solidification of ternary systems where a decrease in one solute results in an increase in the other *via* tie line shifting. Pure Ag was selected for the base metal in part due to the diffusivity of Au and Cu into Ag.<sup>[31,32]</sup> The selection was also made because oxides of Ag are reduced at the bonding temperature and no intermetallics are formed along any possible diffusion paths in the solid. This ideal system simplifies the analysis.

### IV. EXPERIMENTAL METHODS

Observations from the binary Ag-Cu system<sup>[11]</sup> show that in order to quantify the isothermal solidification kinetics using DSC, the isothermal hold temperature must be sufficiently higher than the eutectic temperature to fully resolve the DSC peaks. In this case, the eutectic temperature is 1040 K (767 °C) and an isothermal hold temperature of 1073 K (800 °C) was selected. This represents a superheat of 33 K (33 °C), which is larger than that used in the Ag-Cu binary case [1073 K (800 °C) to 1053 K (780 °C) = 20 K (20 °C)].<sup>[11]</sup> The bonding temperature was selected because the Gibbs' isotherm for

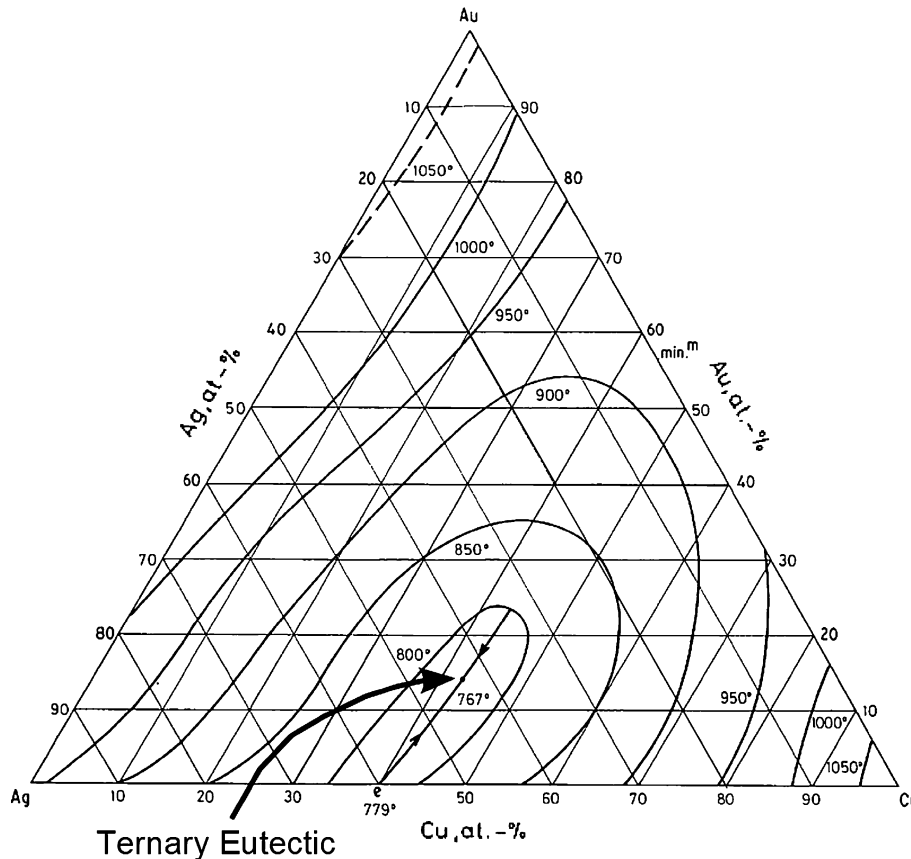


Fig. 3—Liquidus projection of Ag-Au-Cu system.<sup>[34]</sup>

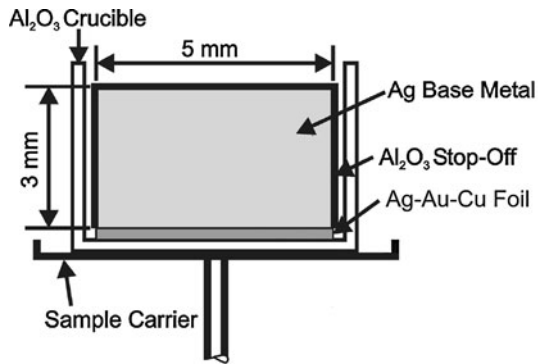


Fig. 4—A typical cross section of the experimental setup within the DSC sample carrier. The Ag cylinder is coated with a ceramic stop-off and placed on a disk of foil.

Ag-Au-Cu at 1073 K (800 °C) is available; furthermore, this temperature allows comparison with the binary Ag-Cu isothermal solidification kinetics.<sup>[11]</sup> Increasing the superheat has been shown to increase the dissolution by the interlayer and the amount of primary solidification that occurs upon cooling, which is expected to have a minor effect on the uncorrected DSC results.

The experimental setup follows that of Kuntz *et al.* as shown in Figure 4.<sup>[11]</sup> Pure Ag base material was purchased from Alfa Aesar in the form of a 5-mm-diameter rod with a purity of 99.95 pct. Right cylinders were cut from these rods to a height of 3 mm. The faying surface of each cylinder was ground flat to 1200 grit paper and they were then cleaned ultrasonically in acetone. To insure wetting only occurred on the faying surface, the side of the cylinder was coated with an alumina lubricant prior to joining.

The interlayer composition for the solid/liquid diffusion couples was the ternary eutectic composition (Ag-27 wt pct Au-27 wt pct Cu). The interlayer foils were prepared by melting a mixture of pure metal powders in an alumina crucible in a DSC. The resulting ingot was formed into a flat disk with a hydraulic press. This disk was rolled into a foil in a series of steps of approximately 50 pct reduction with a recovering annealing schedule in between rolling steps. When the required thickness was achieved, circular disks with a diameter of 5 mm were punched from the foil and weighed. A result of the manual foil preparation method is that each heat had a different nominal thickness. In this case, there were 3 different heats—one thick and two thin—resulting in foils with the following nominal thicknesses: 21.3, 25.4, and 40.6  $\mu\text{m}$ . Only interlayer foils from the same heat were used to compare isothermal solidification kinetics in solid/liquid diffusion couple experiments.

A TLP “half-sample” composed of the base metal and Ag-Au-Cu interlayer was placed in an alumina DSC crucible. A plain Ag slug was placed in the reference crucible so that the thermal properties of both cells would be similar. The TLP half-sample is half of a TLP joint divided at the centerline. This approximation of a TLP joint was designed so that the liquid zone was nearest the measuring thermocouples. The kinetics of the process will not be affected by this setup due to the symmetry of the joint. An issue that may arise is

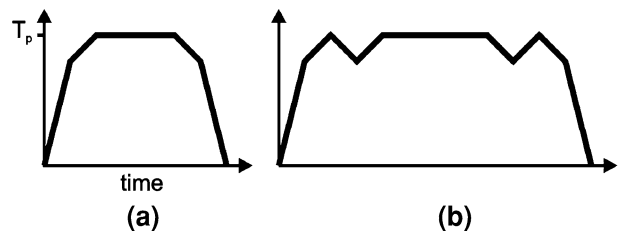


Fig. 5—Temperature programs: (a) type-1 and (b) type-2.

evaporation of the Cu solute as presented by MacDonald and Eagar.<sup>[33]</sup> In the current experiments, the effect of vaporization is expected to be minimal due to negligible partial equilibrium vapor pressure of Cu at the isothermal hold temperature.

A Netzsch 404C differential scanning calorimeter was used for the experiments.<sup>[11,18]</sup> Dynamic nitrogen atmosphere was used in the DSC for all trials to protect the joint from oxidation at elevated temperatures. At 700 C, the heating rate was reduced to 10 °C/min for enhanced measurement resolution and reduced thermal lag in the temperature range of interest. The cooling rate in the region of interest was 10 °C/min. The hold time was varied from zero to near completion for the experiments.

#### A. Temperature Profile for TLP Analysis

Following the experimental procedure from Kuntz *et al.*, two different types of temperature programs seen in Figure 5 were used for the solid/liquid diffusion couples.<sup>[11]</sup>

The type-1 program is composed of a heating stage, an isothermal solidification hold temperature, and a cooling stage. The type-2 program was developed by Kuntz *et al.* to account for several factors including primary solidification and baseline shift that lead to errors in the results.<sup>[11]</sup> Primary solidification is the solidification of the fraction of the liquid that has drifted from the eutectic composition *via* tie line shifting. The preliminary cycle is designed to remove the effects of baseline shift during melting by establishing an interface with a stable thermal conductivity. This was done without having a significant effect on the process kinetics due to their relatively slow rate. To characterize the isothermal solidification, an additional thermal cycle was appended to the end of the heating schedule in order to provide more data. This heating cycle is valuable because it adds a heating segment after the isothermal hold period. Thus, the enthalpy of the eutectic melting endotherm can be measured before and after the isothermal hold period. Correction factors developed with the type-2 program will be applied to the type-1 data and compared with type-2 data to validate the use of the correction method.

Typical DSC traces for the ternary solid/liquid diffusion couples are shown in Figures 6 and 7 for the two different temperature programs. A single peak exists for both melting (endotherm) and solidification (exotherm). The peak corresponds to the eutectic in both cases. Undercooling effects have led to a difference in

melting and solidification temperatures. In Figure 7, the MX and SX values refer to solidification and melting enthalpies for the cycle number.

### B. Enthalpy measurement method

The melting endotherm for a ternary solid/liquid diffusion couple in Figure 6 shows a shift in the baseline across the endotherm. This is also seen in the first cycle of the type-2 temperature program from Figure 7. There are a variety of methods available in the software to integrate the peaks in the presence of a baseline shift such as linear, tangential sigmoidal, horizontal sigmoidal, and horizontal—left or right starting. In the linear case, the peak is integrated between the DSC trace and a line with endpoints on the DSC trace at the integration limits. The equation for the baseline is given by Eq. [4], where  $B(t)$  is the baseline,  $D(t)$  is the differential signal, and  $t_s$  and  $t_f$  are the start and end time of the peak (*i.e.*, integration limits), respectively.

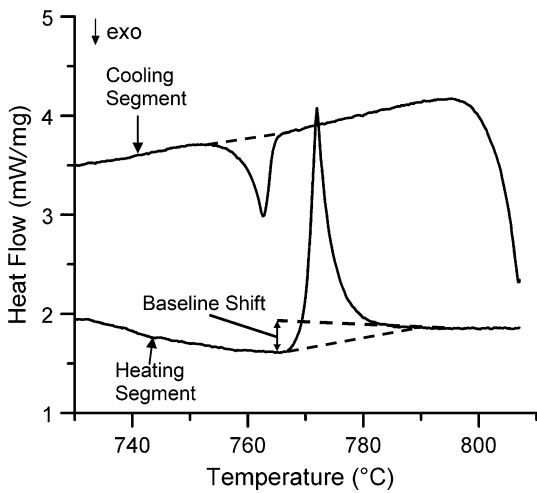


Fig. 6—Typical DSC trace as a function of temperature for type-1 temperature program.

$$B(t) = D(t_s) + (D(t_f) - D(t_s)) \times \frac{t}{t - t_s} \quad [4]$$

In this study, the linear baseline correction method is used exclusively as shown in Figure 8. The baseline shifts occurring in the DSC results of solid/liquid diffusion couple experiments are only visible during the first melting segment and are related to the change in heat transfer condition as discussed in a later section. These baseline shifts cannot be attributed to a change during reaction or temperature dependence of the interlayer-specific heat alone. Acknowledging this, the nature of the needed baseline correction is unknown; thus, a linear interpolation scheme is used.

Integration of an endotherm or exotherm peak requires manual selection of the range to integrate over. The integration limits are determined by examination of the first and second derivatives of the DSC trace. The start of a peak can be considered the temperature where the DSC and the first and second derivative curves start to increase in Figure 9. Recognizing the end of the peak is made difficult when a baseline shift occurs across the peak; however, selection of the limits has a significant effect on the measured enthalpy. The end of the peak is determined by the temperature where the second derivative of the DSC trace returns to zero. At this point, the slope of the trace is no longer changing and the baseline can be said to be reestablished after the thermal event. There is expected to be some measurement error with

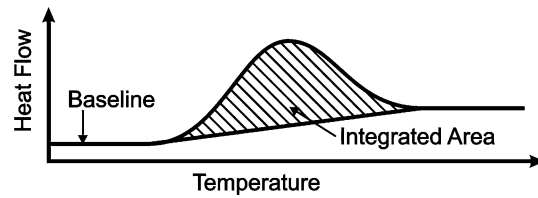


Fig. 8—Baseline correction method for current study.

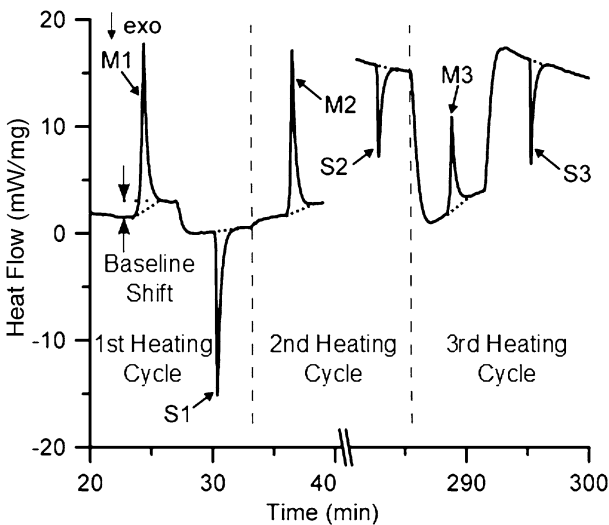


Fig. 7—Typical DSC trace as a function of time for type-2 temperature program.

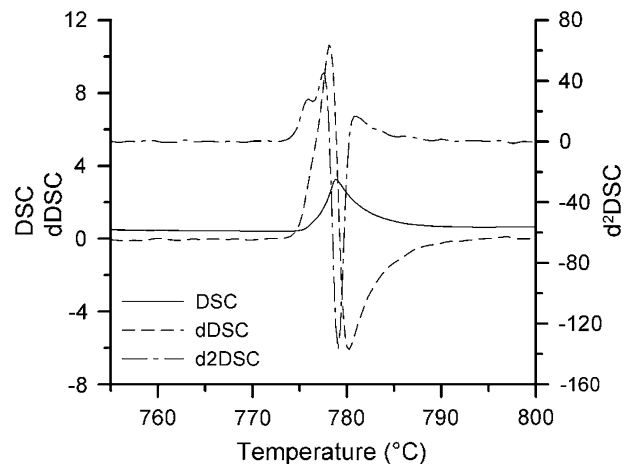


Fig. 9—Melting endotherm of a DSC trace for a solid/liquid diffusion couple showing the first and second derivatives of the DSC curve with respect to time.

determining the limits of integration manually. Using this procedure gives the most consistent results.

### C. Correction Factor

There are a number of effects that have contributed to a systematic underestimation of the percentage of liquid remaining.<sup>[11,18]</sup> The mass ratio of the foil interlayer to base metal is less than 1 percent, causing the measured enthalpy to be lower than without base metal.<sup>[18]</sup> In addition, the base metal acts as a heat sink in the sample, reducing the total heat of formation. The TLP half-sample limits any temperature gradients by having only 1 bond interface, likely minimizing the impact of the base metal on the process kinetics. These effects will vary as the base metal mass varies between samples. With increasing isothermal hold time, the magnitude of the solidification exotherm is expected to decrease as the liquid width decreases.<sup>[18]</sup> Analysis of the isothermal solidification kinetics in the solid/liquid diffusion couples can be performed by taking a ratio of the solidification exotherm ( $\Delta H_s$ ) to the melting endotherm ( $\Delta H_m$ ) as measured in each DSC trial as shown in Eq. [5].<sup>[18]</sup> In this calculation, the heat flow influence from the base metal is consistent during both the melting and solidification events.

$$\text{Pct liquid remaining} = 100 \times \frac{\Delta H_s}{\Delta H_m} \quad [5]$$

A baseline shift occurs in the data due to a change in the thermal resistance of the cell as the foil melts and wets the base metal and bottom of the crucible.<sup>[18]</sup> This results in an overestimation of the melting endotherm ( $\Delta H_m$ ), leading to a decrease in the fraction of liquid remaining calculated. The first cycle was added to the type-2 program to remove this effect. In Figure 6, it can be seen that there is no baseline shift during the second or third cycle. The second cycle is more accurate than the first cycle. The effect of the baseline shift can be quantified by comparing the initial and secondary melting enthalpies with the ratio  $M1/M2$  (mJ/mJ).<sup>[18]</sup>

There is no separate melting peak for the base metal dissolution.<sup>[18]</sup> The presence of the base metal will tend to increase thermal lag, broadening the melting peak of eutectic. This increase in time may have resulted in the endothermic energy of dissolution of the base material being included in the initial peak. This exclusion of a fraction of the base metal dissolution will lead to an error in the calculated percent liquid remaining.

Primary solidification occurs *via* epitaxial growth which causes the associated exothermic energy to not be visible on the DSC trace.<sup>[18]</sup> This causes the exothermic enthalpies to always be smaller than the endothermic enthalpies. The exothermic solidification peak is a measure of only the eutectic fraction of the liquid remaining. This effect can be interpreted by comparing adjacent endotherms and exotherms ( $S1/M2$ ,  $S2/M3$ ,  $S3/M3$ ).  $S1/M2$  and  $S2/M3$  are more accurate for this purpose because they compare the melting endotherm with the previous solidification exotherm. This also takes into account the dissolution effect. The  $M1$

endotherm is not included in this analysis because it was introduced to remove the effect of baseline shift. The extent of isothermal solidification can be approximated by comparing the post-isothermal hold solidification enthalpies  $S2/S3$ . This relation can be used to correct for the exclusion of epitaxial primary solidification and dissolution of the base metal from the DSC measurements.

The result of the discussed effects is a systematic underestimation of the fraction of liquid remaining. A correction factor ( $\Psi$ ) was developed by compounding these effects.<sup>[11,18]</sup> This factor is combined with the original DSC results (Eq. [6]) in order to increase the accuracy of the data, where the fraction of liquid remaining extrapolates close to unity at the ordinate axis.<sup>[18]</sup>

$$\text{fraction of liquid remaining} = \psi \frac{\Delta H_s}{\Delta H_m} \quad [6]$$

The initial interlayer composition, the heating rate, the reference crucible contents, and the base metal coating will be considered in development of the experimental parameters using the aforementioned temperature programs. In addition, the effects of heat conduction into the base metal, baseline shift across the initial melting endotherm, and the exclusion of primary solidification upon cooling combine to systematically reduce the measured fraction of the liquid remaining. These effects have been quantified in the present work using the type-2 temperature program.

## V. Ag-Au-Cu SOLID/LIQUID DIFFUSION COUPLE RESULTS

The DSC results for the ternary solid/liquid diffusion couples agree with the observations from the binary experiments.<sup>[11]</sup> Primary solidification, which is expected to occur upon cooling from the isothermal hold temperature, does not appear as a solidification exotherm on the DSC trace; and, this is expected to influence the DSC results. Baseline shift upon melting of the interlayer is observed and is expected to result in an increase in the measurement of the endotherm. With increasing isothermal hold time, the magnitude of the solidification exotherm is expected to decrease as the liquid width decreases. Thus, analysis of the isothermal solidification kinetics in the solid/liquid diffusion couples can be performed using a method similar to the binary case by taking a ratio of the solidification exotherm to the melting endotherm.<sup>[11]</sup> The type-1 DSC results for the 40.6- $\mu\text{m}$  (thick) Ag-Au-Cu interlayer are shown in Figure 10. Similarly, the type-1 DSC results for the 21.3- $\mu\text{m}$  (thin) ones are shown in Figure 11. As expected, examination of the fraction of liquid remaining shows a systematic decrease with increased isothermal hold time in both the thick and thin foils.

The percentage of liquid remaining in the solid/liquid diffusion couple as calculated by Eq. [6] is shown as a function of the square root of the isothermal hold time. As in the binary case, the liquid width is shown to

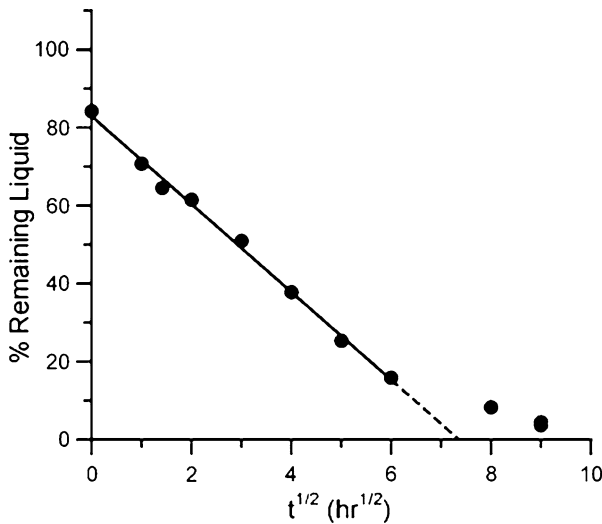


Fig. 10—Type-1 DSC results for thick foil Ag-Au-Cu diffusion couples.

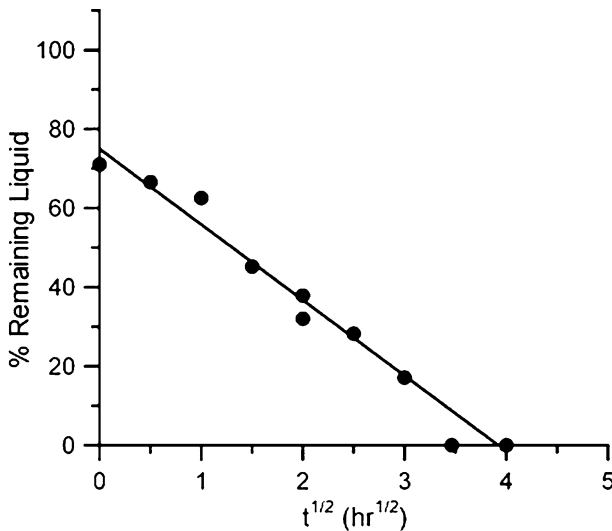


Fig. 11—Type-1 DSC results for thin foil Ag-Au-Cu diffusion couples.

decrease in a manner proportional to the square root of the isothermal solidification time throughout most of the isothermal solidification period.<sup>[11]</sup> Another similarity with the binary case is that the linear trend line does not intersect the ordinate axis at unity, but instead shows an apparent loss of liquid at short isothermal hold times.<sup>[11]</sup> In the binary DSC experiments, this was shown to be an experimental artifact which was revealed by use of the type-2 temperature program.<sup>[11]</sup>

At longer isothermal hold times, the interface kinetics appears to decrease. This is apparent after 36 hours at the bonding temperature. The linear regression trend line shown in Figure 10 is fit only to the data from 0 to 36 hours. The extrapolation to the abscissa is shown by the broken line. The data that lie above the fit line deviate from the linear trend and are excluded from the fit. Time for the completion of isothermal solidification is predicted in the binary case by extrapolating the linear

trend line to the abscissa, where the fraction of liquid remaining is zero. In Figure 10, the two outlying points are excluded from the analysis; hence, the uncertain extrapolation given by the broken line is not an accurate prediction of the isothermal solidification time. A second fit could be applied to the points from 36 hours onward to give good prediction of the time at which the liquid phase is eliminated. The deviation from the linear relationship between the interface position and the root of time is a possible indication of the existence of a second regime of interface kinetics as suggested by the literature.<sup>[27]</sup> In this case, each kinetic regime is dependent on a separate solute differing in diffusivity and/or solubility in the Ag solvent. The observed kinetics follows the theory of isothermal solidification in a ternary system. The type-1 solid/liquid diffusion couple interface kinetics for the thin foil in Figure 11 shows that the fit line does not approach unity at zero isothermal hold time and is consistent with the binary system results.<sup>[11]</sup>

The apparent shift in interface kinetics that was observed with the thick foil in Figure 10 is not clear in the thin foil results (Figure 7). Instead, a linear fit applied to the non-zero points in Figure 11 correlates with the data over the entire range. In both Figures 10 and 11, the characteristic deviation of the abscissa intercept indicates that, like in binary isothermal solidification, the artifacts of the DSC experiments must be corrected.<sup>[11]</sup> It has already been shown that a set of type-2 temperature program DSC experiments can be used to correct the interface kinetics measured using type-1 experiments as well as collect additional data that can be utilized to characterize isothermal solidification. The results of the type-2 solid/liquid diffusion couple DSC experiments for thin foils are summarized in Table 1 and Figure 12.

The interface kinetics as measured using  $S2/M1$  shows similar results to those measured using the type-1 temperature program for a thin foil (Figure 11) with slight differences attributed to a variation in initial thickness between the two heats of foil used for each set of diffusion couples. The nature of the ternary diffusion couple results in Figure 12 compares very well with the binary results.<sup>[11]</sup> Using the data, there are a number of additional methods which can be used to interpret the results.

From the results in Figure 11, an average value for the effect of baseline shift on the initial heating cycle can be found.<sup>[11]</sup> This value is given by the average  $M1/M2$  and is found to be 1.19, compared to 1.24 for the binary Ag-Cu results.<sup>[11]</sup> The effect of primary solidification and dissolution can be found using the average  $M/S$  ratio, which is found to be 1.13, compared to 1.10 for the binary results.<sup>[11,18]</sup> Following the methodology from Kuntz *et al.*, the correction factor ( $\Psi$ ) for the ternary DSC measurements is found to be 1.34.<sup>[18]</sup> This compares to the value of  $\Psi = 1.36$  for the binary results.<sup>[11]</sup> The correction factor is applied to the  $S2/M1$  data from Table 1 with the results given in Figure 13. Similarly, the correction is applied to the type-1 results for both thin (*i.e.*, Figure 11) and thick (*i.e.*, Figure 10) foils in Figures 14 and 15, respectively. The corrected

**Table I. Type-2 DSC Results for Thin Ag-Au-Cu Solid/Liquid Diffusion Couples (enthalpies are in mJ)**

$\sqrt{t}$ (h <sup>1/2</sup> )	M1	S1	M2	S2	M3	S3	M2/M1	S2/M3
0.50	469	366	394	323	361	331	0.84	0.90
1.00	459	338	362	265	286	274	0.79	0.93
2.00	453	351	375	197	214	190	0.83	0.92
3.00	449	361	392	121	137	118	0.87	0.88
4.00	450	358	389	27.0	33.0	24	0.87	0.81

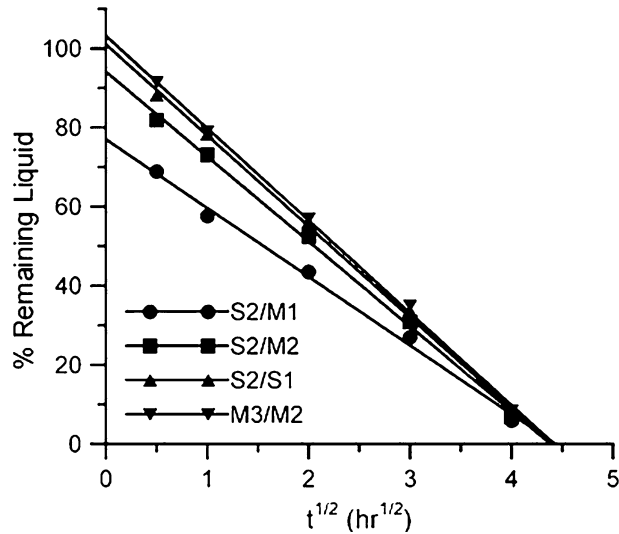


Fig. 12—Ag-Au-Cu diffusion couple thin foil type-2 temperature program results.

fraction of liquid remaining for both of the thin foils (Figures 13 and 14) passes through nearly 100 pct at zero isothermal hold time. The corrected results for the thick foil case, however, deviate by over 10 pct. This is likely a result of the different initial foil thickness and suggests that the effect of baseline shift could be dependent on the thickness of the foil. As in the binary case, the solid/liquid diffusion couple interface kinetics can be quantified using the similar peak data in Table I.<sup>[11]</sup> Figure 16 shows a comparison of the corrected results using the ratio of solidification exotherm to melting endotherm ( $S/M$ ) and the results using similar peaks (*i.e.*,  $M3/M2$  and  $S2/S1$ ). The measured process kinetics is related to the slope of the fit line. Examination of Figure 16 shows that there is good agreement between the techniques. This agrees with the binary case.<sup>[11]</sup> Either of the methods can be used to quantify interface kinetics with the same result.

The corrected line in Figure 16 is derived on the application of a constant correction factor,  $\Psi$ . The assumption that  $\Psi$  is constant may not be valid throughout isothermal solidification in ternary systems. In theory, isothermal solidification proceeds with a shifting liquid composition. Any change in the liquid composition is likely to have an effect on the fraction of liquid that solidifies as eutectic during cooling from the isothermal hold temperature. The distance of the liquidus composition from the eutectic composition will influence the extent of primary solidification; thus, any tie line shift on the Gibbs' isotherm could affect the

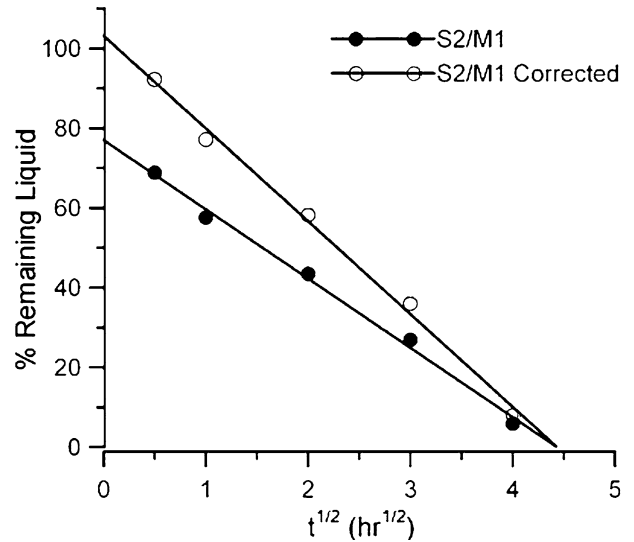


Fig. 13—Type-2 thin foil temperature program results corrected.

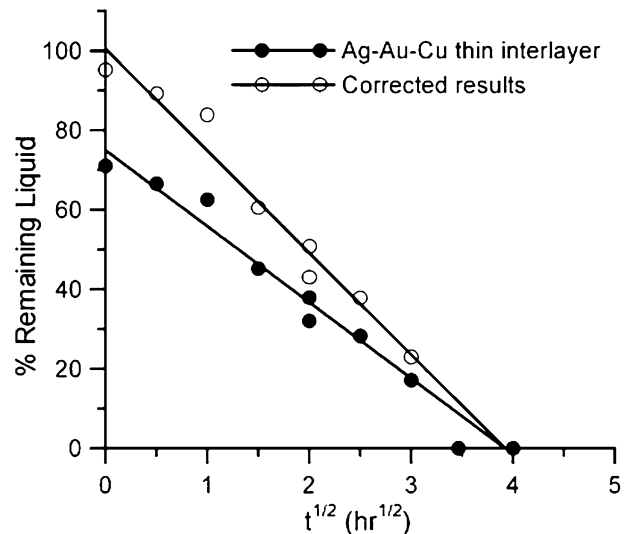


Fig. 14—Type-1 thin foil results corrected.

relationship between the solidification exotherm and melting endotherm. In binary isothermal solidification, the composition of the liquid remains constant throughout isothermal solidification. The ratio of adjacent melting and solidification peaks can be considered constant with time. In the ternary case, however, the assumption that the liquid composition is shifting throughout isothermal solidification is an indication that the assumption of a constant  $\Psi$  may not be valid.

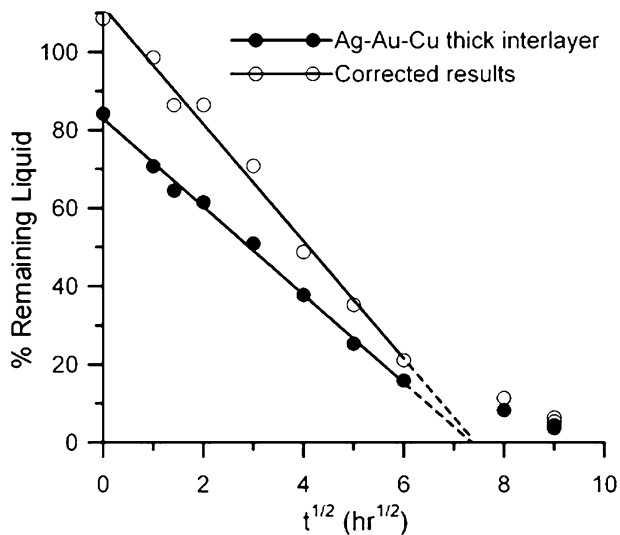


Fig. 15—Type-1 thick foil results corrected.

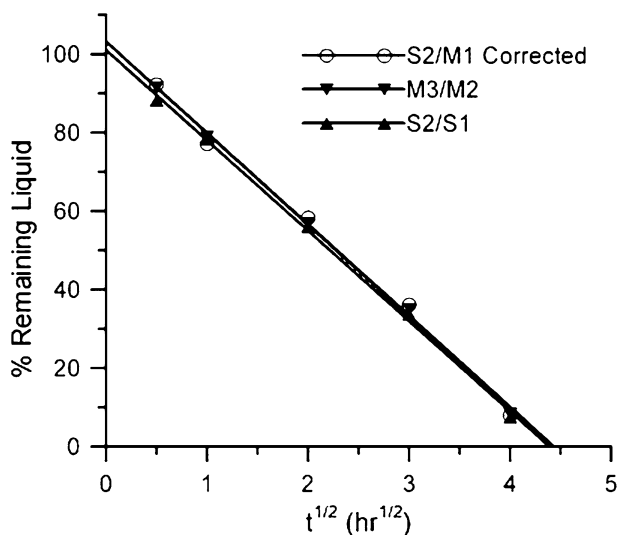


Fig. 16—Comparison of corrected results vs similar peaks.

Closer examination of the endotherms and exotherms in Table I shows that the effect of primary solidification on the enthalpy measurements varies with isothermal hold time. The ratio of adjacent solidification exotherms to melting endotherms (see Figure 7) is plotted as a function of isothermal hold time in Figure 17. The value  $S1/M2$  is the exotherm to endotherm ratio before the isothermal hold period. The values  $S2/M3$  and  $S3/M3$  are the exotherm to endotherm ratios after the isothermal hold period. Observation of Figure 17 shows that the exotherm to endotherm ratio before isothermal solidification remains constant as the isothermal hold time for the solid/liquid diffusion couple increases. Trend lines have been added to the figure to increase legibility. This is expected because these enthalpies are measured before the isothermal hold period and the fraction of eutectic melting, and solidification is constant. The enthalpy ratios after the isothermal hold time, however, show a systematic decrease with increasing

progression of isothermal solidification after the first hour.

The average value for the pre-hold enthalpy ratio  $S1/M2$  is 0.93. The post-isothermal hold enthalpy ratio  $S2/M3$  increases initially from 0.90 at 0.25 hours to 0.93 at 1 hour and then decreases to 0.81 at 16 hours. Likewise, the enthalpy ratio  $S3/M3$  initially increases from 0.92 to 0.96 between 0.25 and 1 hour and decreases to 0.75 after 16 hours of isothermal hold time. The shift in the post-hold enthalpy ratios is an indication of changing interface conditions during isothermal solidification when compared to the constant pre-hold ratio. These changing conditions relate to the tie line shift occurring as isothermal solidification proceeds. The solidus and liquidus concentrations at the interface influence the fraction of eutectic solidifying upon cooling.

The slight increase followed by the systematic decrease in the exotherm to endotherm enthalpy ratio supports the theory that isothermal solidification proceeds in ternary systems by means of a shifting tie line on the Gibbs' isotherm. The results indicate that the liquid composition initially shifts closer to the eutectic (up to one hour) and then moves away from the eutectic until completion of isothermal solidification. The implication of the shifting tie line and change in enthalpy ratio (*i.e.*, change in primary solidification effect) is that  $\Psi$  is shifting throughout isothermal solidification. If the correction factor is obtained at each data point by multiplying the average baseline correction factor (*i.e.*, average  $M1/M2$ ) by the local primary solidification factor (*i.e.*,  $M3/S2$ ), a shifting correction factor can be obtained. This correction factor is plotted as a function of the square root of time in Figure 18. A trend line has been added to the figure to increase legibility. The individual data points in Figure 12 ( $S2/M1$ ) are corrected using the shifting values of  $\Psi$  and plotted in Figure 19.

A comparison of the data correction methods is shown in Figure 19. There is a slight difference between the interface kinetics obtained using the average correction and the shifting correction as shown by slopes of the lines. The results obtained with the shifting correction come slightly closer to 100 pct liquid remaining at zero isothermal hold time; however, the results between the two are insignificant. At longer isothermal hold times when the correction factor value increases well above the average value, the fraction of liquid remaining decreases such that the magnitude of the net change in value becomes quite small. Hence, any influence of the shifting correction is minor.

Based on these results, the use of an average correction factor compares very well with the use of a unique value of  $\Psi$  for each data point. Thus, for the type-1 Ag-Au-Cu DSC experiments, the results can be corrected with an average factor with acceptable results. This allows comparison of results for different initial conditions with the same factor and is useful when local correction data from a type-2 experiment are not available. In this way, any of the three methods can be used to accurately quantify the solid/liquid interface kinetics. Taking a ratio of similar peaks, such as  $S2/S1$  or  $M3/M2$ , yields results that are similar to the ratio of

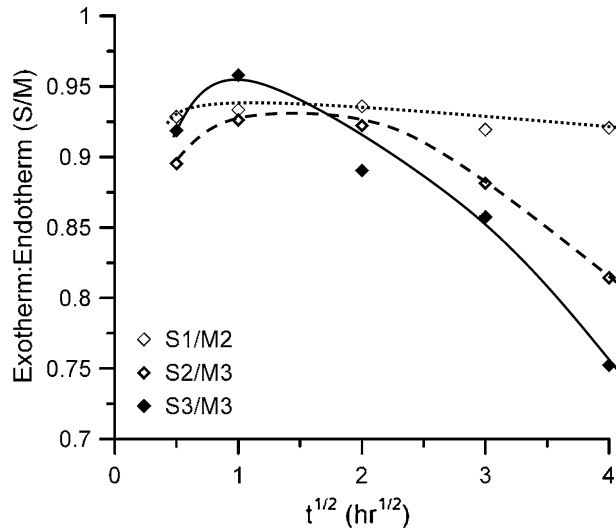


Fig. 17—Observation of changing effect of primary solidification during isothermal solidification in the DSC results.

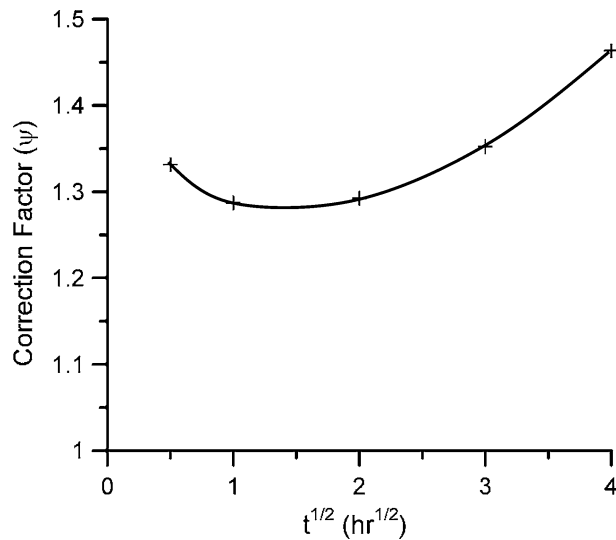


Fig. 18—Shifting correction factor for Ag-Au-Cu solid/liquid diffusion couples.

exothermic enthalpy after isothermal hold time to endothermic enthalpy before (*i.e.*,  $S2/M1$  corrected).

Using the average correction, and a normalization procedure for comparing solid/liquid diffusion couples with different initial foil thicknesses, the results from Figure 13 (type-2 thin foil), Figure 14 (type-1 thin foil), and Figure 15 (type-1 thick foil) can be compared. This comparison is shown in Figure 20. The process kinetics described by each of the lines is similar and compares well with each other. The normalized time is given by Eq. [7], where  $W_{max}$  is the maximum liquid width at the bonding temperature.

$$\sqrt{t^*} = \frac{2 \cdot \sqrt{t}}{W_{max}} \quad [7]$$

Direct comparison of the interface kinetics in Figure 20 allows examination of the apparent change

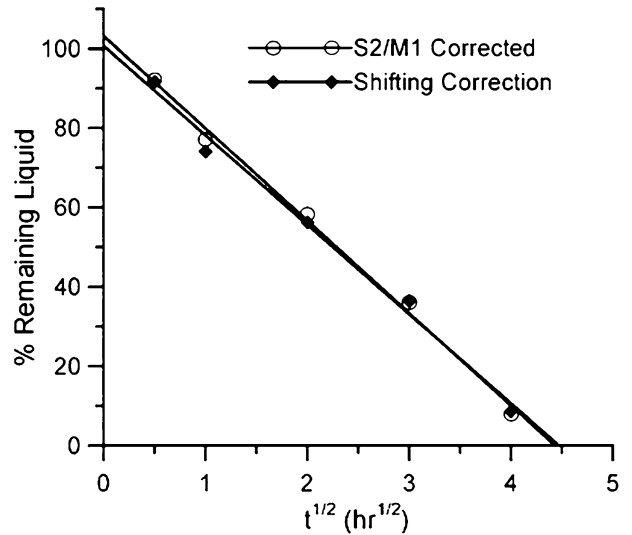


Fig. 19—Ag-Au-Cu solid/liquid diffusion couple type-2 thin foil results, average correction factor, and shifting correction factor.

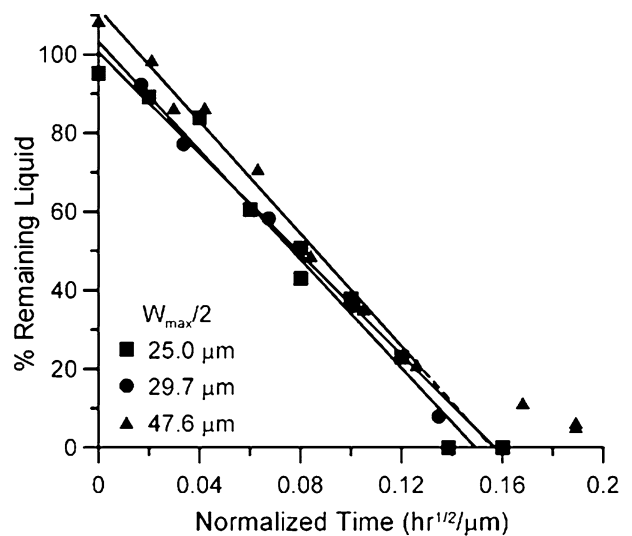


Fig. 20—Normalized Ag-Au-Cu diffusion couple results.

in interface kinetics for the thick foil first shown in Figure 10. The shift in interface kinetics does not appear in the results for the thin foil cases. It is unclear why the second kinetic regime occurs in only the thick foil case; one possibility is that the measurement resolution is not high enough to observe the slight decrease in the interface velocity. Figure 21 shows how the absolute final enthalpy of solidification ( $\Delta H_s$ ) decreases with isothermal hold time for both the thick and thin foil interlayers. It is clear that the absolute  $\Delta H_s$  is significantly larger for the thicker case, as expected. At longer isothermal hold times, the interface velocity decreases in a way that would suggest saturation of the base metal; however, this is not expected due to the ratio of masses between the foil and base and previous modeling.<sup>[26]</sup>

The kinetics of isothermal solidification in binary systems can be compared to those in ternary systems.

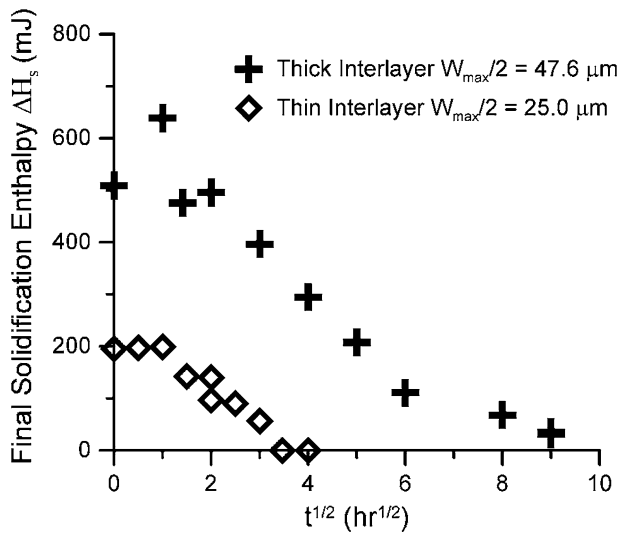


Fig. 21—Comparison of the absolute final solidification enthalpy,  $\Delta H_s$ , for thick and thin interlayers.

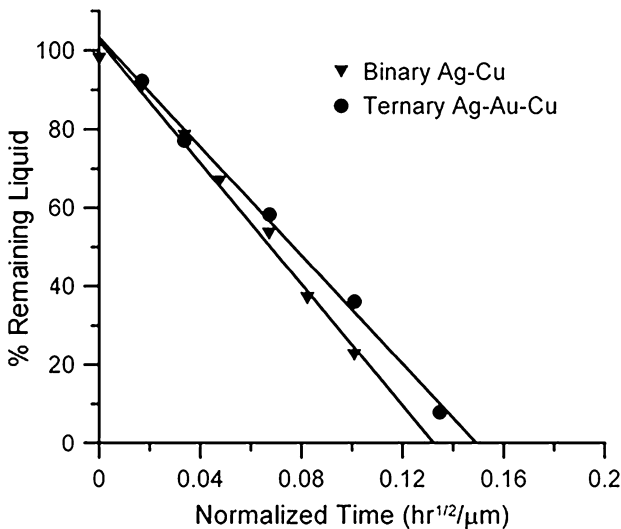


Fig. 22—Comparison of normalized (for  $W_{max}$ ) interface kinetics in binary and ternary diffusion couples.<sup>[11]</sup>

The results can be normalized for interlayer thickness; however, it is not possible to normalize for the chemical difference in liquid composition. Nevertheless, the ternary Ag-Au-Cu results can be compared with the binary Ag-Cu results as both experiments were completed at the same isothermal hold temperature of 1073 K (800 °C). The comparison, shown in Figure 22, reveals that the process kinetics for the binary Ag-Cu solid/liquid diffusion couple with a eutectic interlayer is slightly faster than the interface kinetics for the ternary eutectic Ag-Au-Cu system at the same temperature.

## VI. CONCLUSIONS

The DSC method for quantifying solid/liquid interface kinetics during isothermal solidification has been applied to ternary alloy solid/liquid diffusion couples.

Eutectic Ag-Au-Cu foil interlayers were coupled with pure Ag base metal to study the effects of an additional solute on interface motion. As in the binary case, experimental artifacts including baseline shift and primary solidification contribute to a systematic underestimation of the fraction of liquid remaining.<sup>[17]</sup> A type-2 temperature program has been employed to quantify and empirically correct these effects.

The corrected results, as well as those obtained using similar peaks, show a fraction of liquid remaining that decreases linearly with the square root of time. This infers that a single interface rate constant can be applied to the results over the entire duration of isothermal solidification. The measured interface kinetics is independent of the measurement method, whether it is a corrected ratio of exotherm to endotherm or a ratio of similar peaks. The interface kinetics is also independent of the initial interlayer thickness as normalized results show a similar interface rate constant.

The application of a constant correction factor to the DSC results is made under the assumption that the experimental artifact of primary solidification is not changing as isothermal solidification progresses. Isothermal solidification when more than one solute is present occurs *via* shifting tie line compositions at the solid/liquid interface. The DSC results show that the fraction of liquid solidifying in the primary phase changes with isothermal hold time. As isothermal solidification progresses, the effect of primary solidification on the DSC results increases. Application of a correction factor that changes according to the effect of primary solidification may be appropriate; however, in the Ag-Au-Cu results, the difference in interface kinetics with a static correction factor is minimal. By comparing similar peaks, the experimental artifacts can be removed from the measurement. The results show no difference between the measurement methods. Thus, in this case, all methods are suitable.

## ACKNOWLEDGMENT

This study has been supported by the Ontario Centres of Excellence and the Natural Science and Engineering Research Council.

## REFERENCES

1. D. Duvall, W. Owczarski, and D. Paulonis: *Weld. J.*, 1974, vol. 53, pp. 203–14.
2. G. Cook and C. Sorensen: *J. Mater. Sci.*, 2011, vol. 46, pp. 5305–23.
3. T. Eager and W. Baeslack: *Encyclopedia of Advanced Materials*, D. Bloor, M. Flemings, R. Brook and S. Mahajan, eds., Pergamon Press, Oxford, 1994, pp. 1221–25.
4. L. Connor, ed.: *Welding Handbook*, 8 ed., vol. 1, American Welding Society, Miami, FL, 1989.
5. Y. Zhou, W. Gale, and T. North: *Int. Mater. Rev.*, 1995, vol. 40 (5), pp. 181–96.
6. J. Jung and C. Kang: *Mater. Trans. JIM*, 1996, vol. 37 (5), pp. 1008–13.
7. M. Yeh and T. Chuang: *Weld. J.*, 1997, vol. 76 (12), pp. 517s–21s.

8. K. Nishimoto, K. Saida, D. Kim, and Y. Nakao: *ISIJ Int.*, 1995, vol. 35 (10), pp. 1298–1306.
9. W. MacDonald and T. Eagar: *The Metal Science of Joining*, M. Cieslak, J. Perepezko, S. Kang and M. Glicksman, eds., The Minerals, Metals & Materials Society, 1992, pp. 93–100.
10. J. Ramirez and S. Liu: *Weld. J.*, 1992, vol. 71 (10), pp. 365s–75s.
11. M. Kuntz, Y. Zhou, and S. Corbin: *Metall. Mater. Trans. A*, 2006, vol. 37A, pp. 2493–2504.
12. K. Ikeuchi, Y. Zhou, H. Kokawa, and T. North: *Metall. Trans. A*, 1992, vol. 23A, pp. 2905–15.
13. T. Padron, T. Khan, and M. Kabir: *Mater. Sci. Eng. A*, 2004, vol. 385, pp. 220–28.
14. A. Ghoneim and O. Ojo: *Comput. Mater. Sci.*, 2011, vol. 50, pp. 1102–13.
15. A. Rahman and M. Cavalli: *Mater. Charact.*, 2012, vol. 69, pp. 90–96.
16. K. Ohsasa, T. Shinmura, and T. Narita: *J. Phase Equilib.*, 1999, vol. 20 (3), pp. 199–206.
17. S. Corbin and P. Lucier: *Metall. Mater. Trans. A*, 2001, vol. 32A, pp. 971–78.
18. M. Kuntz, S. Corbin, and Y. Zhou: *Acta Mater.*, 2005, vol. 53 (10), pp. 3071–82.
19. R. Venkatraman, J. Wilcox, and S. Cain: *Metall. Mater. Trans. A*, 1997, vol. 28A, pp. 699–706.
20. S. Cain, J. Wilcox, and R. Venkatraman: *Acta Mater.*, 1997, vol. 45 (2), pp. 701–07.
21. Y. Zhou and T. North: *Acta Metall. Mater.*, 1994, vol. 42 (2), pp. 1025–29.
22. Y. Takahashi, K. Morimoto, and K. Inoue: *Trans. JWRI*, 2001, vol. 30, pp. 535–41.
23. J. Niemann and R. Garrett: *Weld. J.*, 1974, vol. 53 (4), pp. 175s–84s.
24. W. MacDonald and T. Eagar: *Annu. Rev. Mater. Sci.*, 1992, vol. 22, pp. 23–46.
25. K. Saida, Y. Zhou, and T. North: *J. Jpn. Inst. Met.*, 1994, vol. 58, pp. 810–18.
26. C. Sinclair: *J. Phase Equilib.*, 1999, vol. 20 (4), pp. 361–69.
27. C. Sinclair, G. Purdy, and J. Morral: *Metall. Mater. Trans. A*, 2001, vol. 31A, pp. 1187–92.
28. P.R. Subramanian and J.H. Perepezko: *ASM Handbook: Alloy Phase Diagrams*, H. Baker, ed., vol. 3, Materials Park, OH, ASM International, 1992.
29. H. Okamoto and T. Massalski: *ASM Handbook: Phase Diagrams of Binary Gold Alloys*, ASM International, Materials Park, OH, 1987.
30. H. Okamoto, D. Chakrabarti, D. Laughlin, and T. Massalski: *ASM Handbook: Phase Diagrams of Binary Gold Alloys*, ASM International, Materials Park, OH, 1987.
31. T. Ziebold and R. Ogilvie: *Trans. Met. Soc. AIME*, 1967, vol. 239 (7), pp. 942–53.
32. Y. Liu, J. Wang, Y. Du, G. Sheng, L. Zhang, and D. Liang: *Comput. Coupl. Phase Diagr. Thermochem.*, 2011, vol. 35, pp. 314–22.
33. W.D. MacDonald and T.W. Eagar: *Metall. Mater. Trans. A*, 1998, vol. 29A, pp. 315–25.
34. A. Prince: *Int. Mater. Rev.*, 1988, vol. 33 (6), pp. 314–38.